

**QUASI - REAL QED COMPTON MONTE CARLO
FOR HERA**

A. COURAU, S. KERMICHE

Laboratoire de l'Accélérateur Linéaire
CNRS - IN2P3 - Université PARIS - SUD
91405 - ORSAY FRANCE

T. CARLI

Laboratoire de Physique Nucléaire des Hautes Energies
CNRS - IN2P3 - Ecole Polytechnique
91128 - PALAISEAU FRANCE

and

P. KESSLER

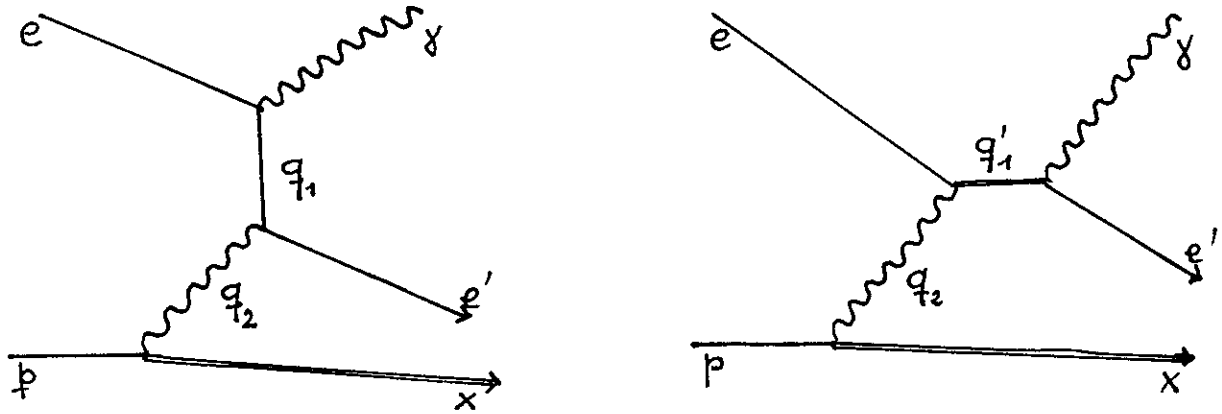
Laboratoire de Physique Corpusculaire
CNRS - IN2P3 - Collège de France
75231 - PARIS FRANCE

Abstract

This paper contains some description and features of an unweighted Monte Carlo of quasi-real QED Compton events obtained in head - on ep collisions. This means the generation of events involving a final state with one electron and one photon, almost coplanar, observed inside the detector at finite angle.

I - DEFINITIONS AND REMARKS

Considering the reaction $ep \rightarrow e\gamma X$ corresponding to the diagrams



- Fig. 1 -

one gets, a priori¹

$$ds \approx \frac{dq_1}{q_1^2 - m_e^2} \cdot \frac{dq_2}{q_2^2}$$

It results that the cross section is largely dominated by both q^2 close to zero. But in this case the outgoing electron and photon, as well as the hadronic system, go along the beam axis and escape the main detector. This configuration corresponds to the so-called **Bremstrahlung** and it leads to a large counting rate, but only in a specific detector for low angles.

Looking for particles at finite angles inside the detector requires at least that one of the two q^2 takes finite values not too close to zero. Then the cross section is dominated by the other q^2 close to zero. One has ~~to~~ consider two different configurations :

i) $q_1^2 (q_1'^2) \rightarrow 0$, q_2^2 finite : then the photon goes straightforward along the incident (Resp. final) electron direction, and we observe the electron and the hadronic system in the detector. This corresponds to the so-called **radiative correction** .

ii) $q_2^2 \rightarrow 0$, q_1^2 finite : The hadronic system goes straightforward, and we observe the electron and the photon in the detector. This corresponds to the so-called **quasi-real Compton process**.

¹ Let us note that in practice the pole in the propagator of the exchanged photon vanishes when both vertices $e\gamma$ and $p\gamma X$ are inelastic.

We call those events quasi-real QED COMPTON since they are dominated by small q_2^2 and therefore they involve the scattering of a quasi-real γ with the incident electron. Note that small q_2^2 actually means small with respect to W^2 where W is the invariant mass of the $e\text{-}\gamma$ system. A priori one selects events with $|q_2^2| \ll W^2$ by looking at coplanar $e\text{-}\gamma$ events observed within the detector.

II - EXACT EXPRESSION OF THE GENERAL CROSS-SECTION

The following expressions are "exact" in the sense that no approximation was introduced a priori in the computation of the Feynman diagrams of the fig. 1. They are unavoidably model dependant to some extent (mainly as far as the inelastic part of the proton's photon spectrum is concerned), but as precise as our experimental and theoretical knowledge allows to be.

Using the helicity amplitudes method the calculation of the Feynman graphs shown in fig. 1 leads to :

$$\frac{d^4\sigma^{pe \rightarrow xe\gamma}}{dx dx' dQ^2 d\Omega^*} = f_{\gamma^*/p}^T(X, X', Q^2) \left[\frac{d\sigma}{d\Omega^*} \right]^T + f_{\gamma^*/p}^L(X, X', Q^2) \left[\frac{d\sigma}{d\Omega^*} \right]^L$$

with :

$$\left(\frac{d\sigma}{d\Omega^*} \right)^T = \frac{d\sigma_T}{d\Omega^*} + \varepsilon \frac{d\sigma_L}{d\Omega^*} + \sqrt{2\varepsilon(\varepsilon+1)} \frac{d\sigma_{TL}}{d\Omega^*} \cos \varphi^* + \varepsilon \frac{d\sigma_{TT}}{d\Omega^*} \cos 2\varphi^*$$

$$\left(\frac{d\sigma}{d\Omega^*} \right)^L = \frac{d\sigma_L}{d\Omega^*} + \frac{1+\varepsilon}{2\varepsilon} \frac{d\sigma_L}{d\Omega^*} + \sqrt{\frac{1+\varepsilon}{\varepsilon}} \frac{d\sigma_{TL}}{d\Omega^*} \cos \varphi^* - \frac{d\sigma_{TT}}{d\Omega^*} \cos 2\varphi^*$$

where the upper subscript (T,L) refers to the virtual photon's polarisation (transverse or longitudinal) at the hadronic vertex and the lower subscript (T, L, TL, TT) refers to the virtual photon's polarisation at the leptonic vertex, i. e. defines the transverse, longitudinal, transverse-longitudinal and transverse-transverse interference terms of the virtual compton cross section $e\gamma^* \rightarrow e\gamma$.

One has the following expressions for the "virtual photon spectra"

$$f_{\gamma^*/p}^T = \frac{1-x}{4\pi^3 x x'} F^T(x, x', Q^2) \sigma_T^{\gamma^* p}$$

$$f_{\gamma^*/p}^L = \frac{1-x}{4\pi^3 x x'} F^L(x, x', Q^2) \sigma_L^{\gamma^* p}$$

where
$$F^L(x, x', Q^2) = F^T(x, x', Q^2) - \frac{x'^2}{2x^2} = \frac{(1-x'/x) Q^2 - x'^2 m_p^2}{Q^2 + 4x^2 m_p^2}$$

and $\sigma_{T(L)}^{\gamma^* p}$ is the transverse (longitudinal) cross section of the virtual photon production process $\gamma^* p \rightarrow X$, where Q^2, x, x' are defined as :

$$Q^2 = -q_2^2 \quad ; \quad x = \frac{-q_2^2}{2p_p q_2} = \frac{Q^2}{m_X^2 - m_p^2 + Q^2}$$

$$x' = \frac{q_2 p_e}{p_p p_e} = \frac{W^2 + Q^2 - m_e^2}{S - m_p^2 - m_e^2} \approx \frac{W^2 + Q^2}{S}$$

calling m_X, m_p, m_e the mass of the final hadronic state, proton and electron and defining

$$W^2 = (q_2 + p_e)^2 \quad \text{and} \quad S = (p_p + p_e)^2.$$

The polarisation parameter ϵ is given by $\epsilon = F^L/F^T$

while the various polarisation terms of the virtual compton scattering are given by :

$$d\sigma_T = \frac{\alpha^2}{W^2 + Q^2} \left[\frac{W^2}{(W^2 + Q^2)(1 + u^* + \eta)} + \frac{(W^2 + Q^2)(1 + u^*)}{4W^2} + \frac{Q^2(1 - u^*)}{W^2(1 + u^* - \eta)} + \frac{Q^2(1 - u^*)}{2(W^2 + Q^2)} \right] d\Omega^*$$

$$d\sigma_L = \frac{\alpha^2}{W^2 + Q^2} \left[\frac{Q^2(1 - u^*)}{W^2 + Q^2} \right] d\Omega^*$$

$$d\sigma_{TL} = -\frac{\alpha^2}{W^2 + Q^2} \left[\frac{QW}{2(W^2 + Q^2)} \left(\sqrt{1 - u^{*2}} + \frac{Q^2}{W^2} \frac{1 - u^*}{1 + u^* + \eta} \right) \right] d\Omega^*$$

$$d\sigma_{TT} = \frac{\alpha^2}{W^2 + Q^2} \left[\frac{Q^2}{2(W^2 + Q^2)} (1 - u^*) \right] d\Omega^*$$

where $d\Omega^* = du^* d\varphi^*$, $u^* = \cos \Theta^*$, Θ^* and φ^* being the orbital and azimuthal scattering angle in the C. of M. frame of the compton scattering process ; η is given by² :

$$\eta = \frac{2m_e^2 W^2}{(W^2 + Q^2)^2}$$

Now, the only parameters that need further specifications are $\sigma_{(\gamma^*p)}^T$ and $\sigma_{(\gamma^*p)}^L$.

Actually, we take into account different contributions according to various range of m_x and Q^2 :

i) Elastic contribution $m_x = m_p$

In this case, we use the following expressions :

$$\sigma_{(\gamma^*p)}^T = \frac{4\pi^2 \alpha}{Q^2} G_M(Q^2) \frac{\delta(1-x)}{1-x}$$

$$\sigma_{(\gamma^*p)}^L = \frac{16\pi^2 \alpha m_p^2}{Q^4} G_E(Q^2) \frac{\delta(1-x)}{1-x}$$

where we take the conventional expressions for the proton's electromagnetic form factors :

$$G_e(Q^2) = \frac{G_M(Q^2)}{2.79} = (1 + Q^2/Q_0^2)^{-2}$$

with $Q_0^2 = 0.71 \text{ GeV}^2/c^2$

ii) Resonant contribution $(m_p + m_\pi) < m_x < 1.8 \text{ GeV}$.

We assume that range to be essentially saturated by the contribution of the three resonances $\Delta(1236)$, $N^*(1520)$, $N(1688)$. From experimental results on electroproduction, one set :

$$\sigma^L = 0$$

$$\sigma^T = \sum_R \sigma_R \frac{W_R^2 \Gamma_R^2}{(m_x^2 - m_R^2)^2 + W_R^2 \Gamma_R^2} \left(1 + \frac{Q^2}{Q_R^2}\right)$$

² We only take into account the electron mass where it is necessary in order to avoid divergency.

where the values of the various parameters are given in the following table.

	Δ	N^*	N^*
M_R (GeV)	1236	1520	1688
σ_R (μb)	550	280	220
Γ_R (GeV)	0.12	0.12	0.12
Q_R^2 (GeV^2/c^2)	2.5	3.0	3.0

iii) Inelastic contribution $m_x \geq 1.8$ GeV.

a) For large Q^2 we use the quark parton model and assuming $\sigma^L = (Q^2 / v^2) \sigma^T$ where $v = Q^2 / 2m_p x$, we get :

$$\sigma_T = \frac{4\pi^2 \alpha}{(1-x) Q^2} F_2^p(x, Q^2)$$

$$\sigma_L = \frac{4\pi^2 \alpha}{(1-x) Q^2} \frac{4x^2 m_p^2}{Q^2} F_2^p(x, Q^2)$$

where $F_2^p(x, Q^2)$ is the classical proton structure function.

b) For Q^2 tends to zero, we simply use the well known cross section of real photon production

$$\sigma_T \approx 100 \mu\text{b}$$

$$\sigma_L = 0$$

c) Finally we set over the full Q^2 range :

$$\sigma_T = \frac{4\pi^2 \alpha}{(1-x) Q^2} F_2^p(x, Q^2) \cdot \phi(x, Q^2)$$

$$\sigma_L = \frac{4\pi^2 \alpha}{(1-x) Q^2} \frac{4x^2 m_p^2}{Q^2} F_2(x, Q^2) \cdot \phi(x, Q^2)$$

where
$$\phi(x, Q^2) = \frac{Q^2 (\text{GeV}^2)}{Q^2 (\text{GeV}^2) + F_2(x, Q^2)}$$

is an interpolation factor which provides a smooth continuous transition between the two Q^2 ranges (noticing that x goes to zero when Q^2 tends to zero and $4\pi\alpha^2 / (1 \text{ GeV}^2) \approx 100 \mu\text{b}$).

III - QUASI-REAL QED COMPTON MONTE-CARLO

As we already noticed, the previous formulae correspond to a general and exact computation of the graphs in Fig. 1. Because of the presence of various poles in the various propagators, it is however impossible to generate at once a Monte-Carlo having the same good accuracy over the whole phase-space and experimental configurations. Here we have chosen the generation of "COMPTON" events, i. e. those **experimental events with one electron and one photon almost coplanar observed at finite angle inside the detector**. Those events are overdominated by small q_2^2 when the limitations on acoplanarity and polar acceptance leads to finite value of q_1^2 and q_1^2 with $q_2^2 \ll W^2$ and³ $\eta \ll (1-u^*)$.

Therefore, in a first step we generate $e\text{-}\gamma$ events inside the detector according to an approximation of the cross-section obtained by neglecting η and Q^2/W^2 in $d\sigma^T/d\Omega^*$ and $d\sigma^L/d\Omega^*$. This is only a dynamical approximation, but all physical quantities (including Q^2) are generated and the kinematic is derived in an exact way. This generation is performed over the whole experimentally available phase space that is first determined from the acceptance of the detector at the beginning of the program.

In a second step, the generated events are weighted by comparing for their given parameters, the value of the differential cross section used in the first step to the value of the "exact" one. This allows us, in principle, to provide an exact Monte Carlo over the whole available phase space. However the more q_2^2/W^2 increases, the larger are the weights of the

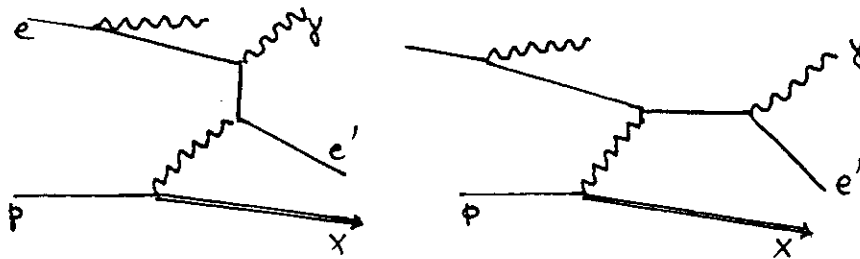
³ The fact that the polar acceptance in the LAB also limits $\cos \theta^*$ in the $e\gamma$ system at rest is not so obvious, but can be proved.

events. Actually, this means that one tends to a second pole regime where q_1^2 becomes smaller than q_2^2 (i.e. we go from the "Compton" to the "radiative correction on the outgoing electron line"). We obviously have to reject events with a large weight for two reasons : the first one is because in this case the statistical accuracy becomes small ; the second one is to be able through a limited increase of the cross section normalisation to get weight smaller than 1 which allows us to provide an output of individual (unweighted) events.

Since the $Q^2 = |q_2^2|$ is strongly correlated to $(\Sigma \vec{p}_t)^2 = Q^2 (1 - W^2/Sx)$ large values of Q^2/W^2 and weights are correlated to the e, γ accoplanarity (see Fig. 2). Thus, the "COMPTON" events with relatively small Q^2/W^2 and weight are selected according to a cut on the $e-\gamma$ accoplanarity angle $(\pi - \Delta\phi) < \alpha \leq 45$ degrees).

The accoplanarity cut leads to limitations on Q^2 and $|\Sigma \vec{p}_t|$ for the overdominant contribution at low W . In the present version of the program, we do not take the diagram of weak interaction into account and we only use structure functions without a Q^2 dependance (e.g. : Schremp-Schremp). However, in order to be precise in any W , range a cut on $\Sigma \vec{p}_t < 20$ GeV must be added.

Radiative corrections to the Compton process affect the cross section as well as the distributions of various parameters. The only significant contribution proceeds from radiation by the incident electron.



Such a contribution is taken into account, in peaking approximation, by introducing a loss of the initial electron's energy according to a probability law given by⁴:

$$d\rho(k) = \beta \cdot k^{\beta-1} (1 - k + k^2/2) dk$$

with : $\beta = \frac{2\alpha}{\pi} \ln\left(\frac{2E}{m_e} - \frac{1}{2}\right)$; $k = E_\gamma/E$

where E is the beam energy of the electron.

⁴ Such a procedure is justified by the fact that the radiated photon and the scattered one emitted at different angles are "distinguishable" and do not interfere.

Note that the hard-photon tail has low probability, but leads to small value of W involving large cross section. The program uses in the generation the resulting value of the electron energy after radiation. However, this radiation leads to weight the events, because the absolute normalisation at the beginning of the program involves the nominal beam energy. The hard photon tail of the γ spectrum can be eliminated to a large extent by imposing a lower limit on the $e\gamma$ visible energy. Such a cut is again necessary and sufficient to get a limited weight.

The hadronic mass is generated but we do not look at possible hadronic components inside the detector. However let us note that as far as the elastic contribution is concerned the proton escapes from the main detector (at finite angle).

Figures 3 to 6 show the distribution of different parameters or "observables" obtained by the Monte Carlo within the following experimental conditions :

$$E_e = 30 \text{ GeV}, \quad E_p = 830 \text{ GeV}$$

$$\pi - |\varphi_{e'} - \varphi_\gamma| < 45^\circ, \quad |(\vec{p}_T)_{e'} + (\vec{p}_T)_\gamma| < 20 \text{ GeV}, \quad E_{e'} + E_\gamma > 20 \text{ GeV}$$

$$E_{e'}, E_\gamma > 2 \text{ GeV}, \quad 3.6 < \theta_{e'}, \theta_\gamma < 176^\circ$$

Figure 7 shows (as an example) the correlated distributions of the $e\gamma$ events inside the H1 subdetectors.

IV - USE OF THE COMPTON GENERATOR

How to run the Compton Generator ?

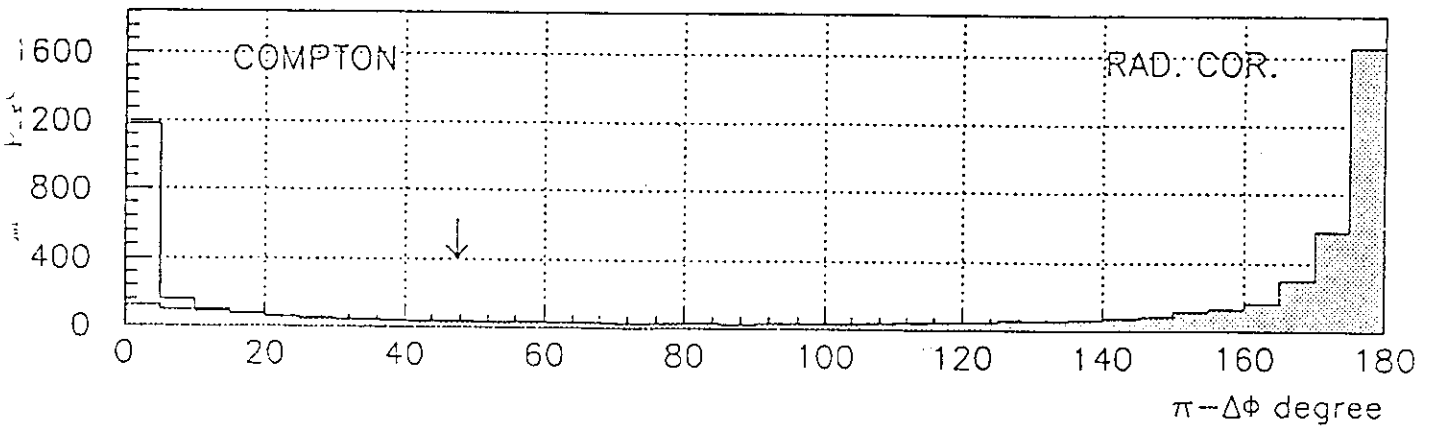
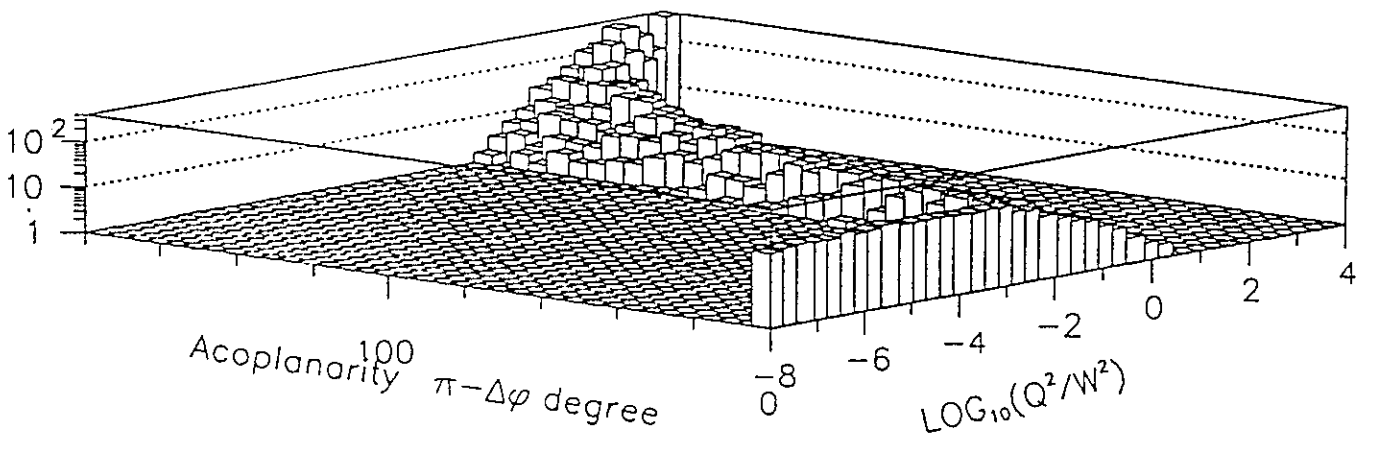
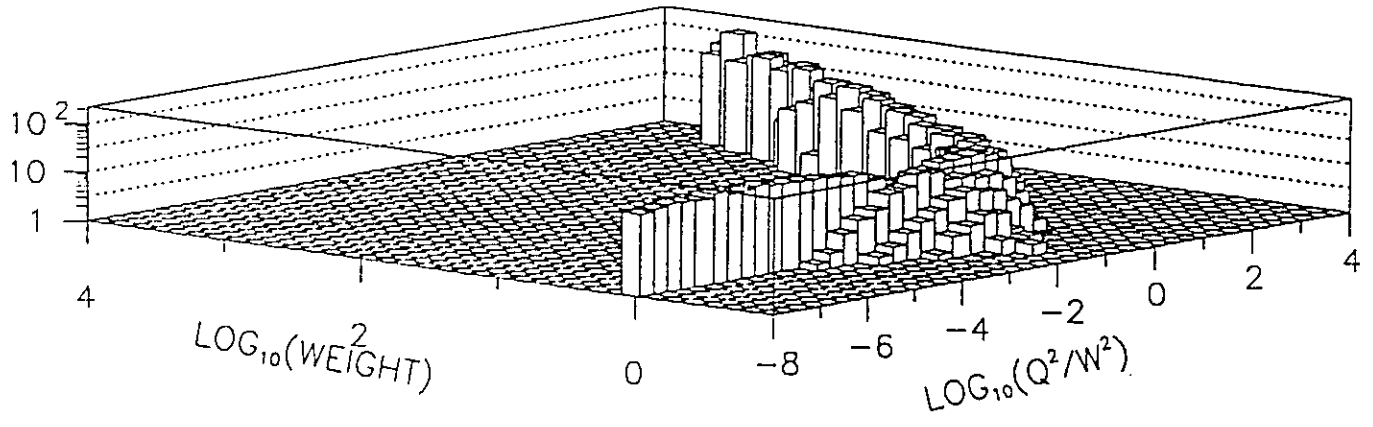
- - User initialisation

The user must choose the following parameters in the steering bank (GCOM) or run one the defaults :

- * Number of events to be generated (NEVENT D = 10)

- * Cuts on polar acceptance (AGMIN D = 3.6, AGMAX D = 176) and acoplanarity (ACO D = 45), if one choose ACO>45 the program automatically set it to 45 degree.

- * Cuts on the minimal value of the outgoing e, gamma energies and the visible energy. (ELIME = 2 GeV, ELIMG = 2 GeV, VMIN = 20 GeV)
 - * Cut on the transverse momentum PTMAX, for the moment the maximal value of PT is 20 GeV. If one chooses PTMAX > 20 GeV, the program automatically resets it to 20 GeV.
 - * Minimal and maximal values of the invariant mass W for the (e-gamma) system, can be chosen for an optimisation of the use of the program in various W range.
- - The user can introduce "radiative corrections" on the incident electron in a collinear approximation by setting LCOR = 1 (D = 0).
Four types of structure functions F2 (x) can be chosen by the option NTYPFF.
 - - The Monte Carlo outputs some histograms. The user can decide if he (she) would like to have these histograms on unit 6 only (NHIST = 1), on a PAW file only (NHIST = 3) or on both the unit 6 and PAW file (NHIST = 2). Those histograms correspond to weighted events, before and after ACO and PT cuts.
 - - If the user would like to produce his (her) own histograms, he (she) can set NHIST = 0 and use a private analysis program in the following files, which are called in the main program and can be found in the CMZ file :
 - GUBEG : for the user initialisation (e. g. PAW or LOOK)
 - GUANA : called after every generation of an event. The user can access the necessary information via the JETSET commons [P(I,J), K(I,J)].
 - GUEND : called after processing the last event.
 - - A new version of the Monte Carlo is foreseen using no cut on PT, but including weak interactions and using the most general structure function depending on Q² (F2(x,Q²)) as well as hadronisation.



(the shadowed area shows the inelastic contribution)

Figure 2

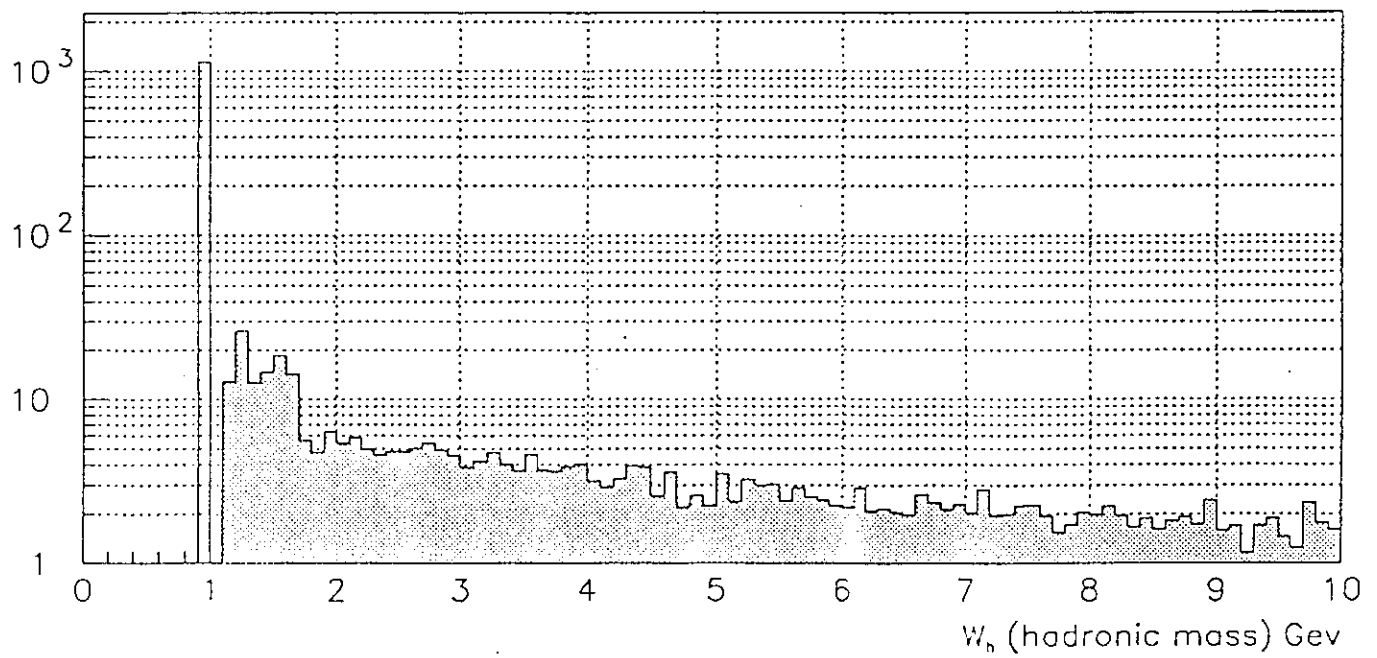
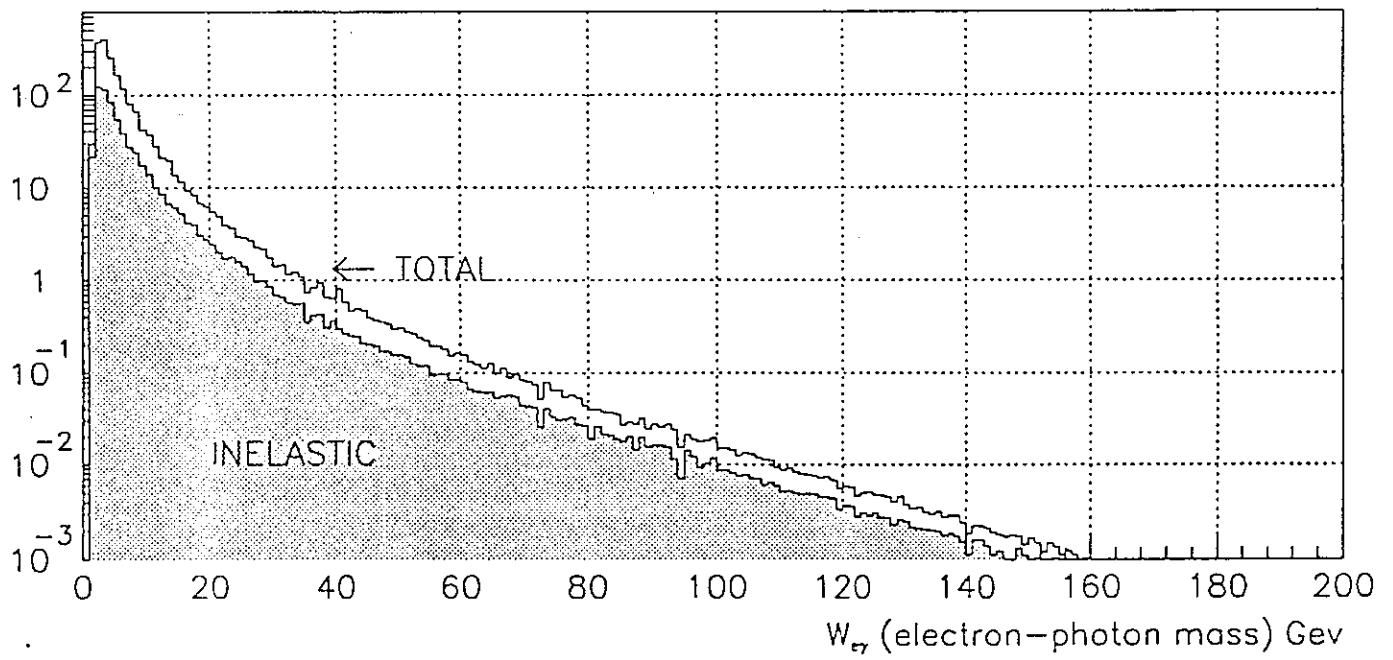


Figure 3

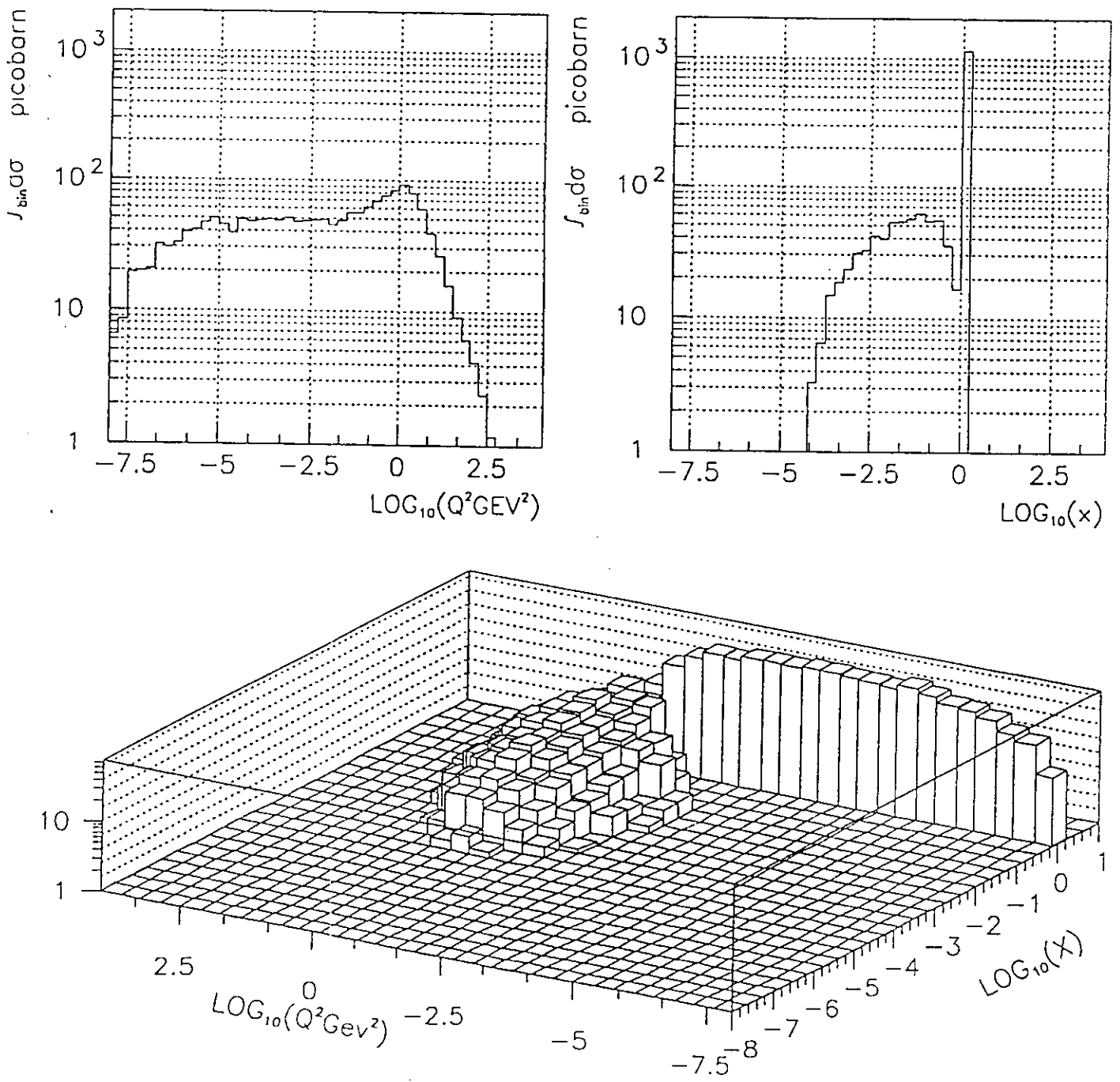


Figure 4

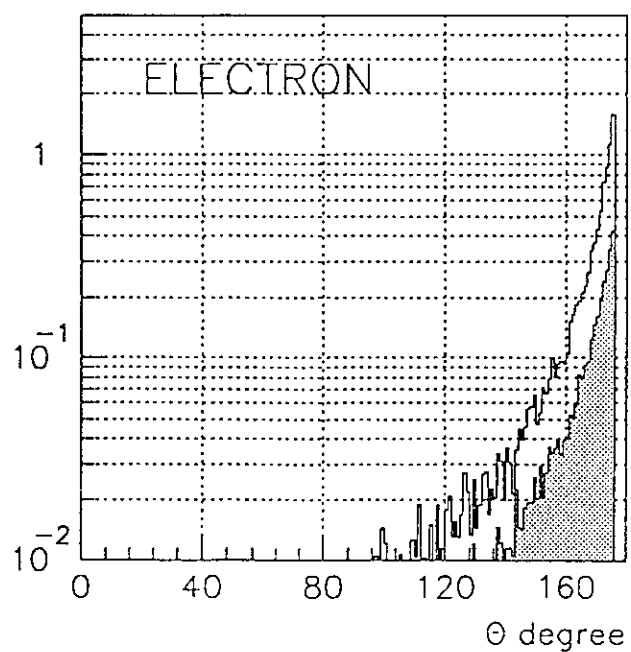
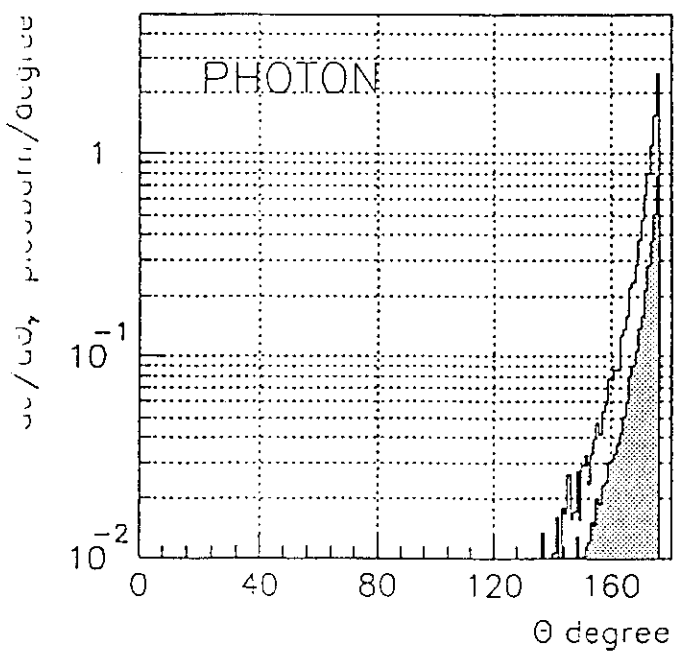
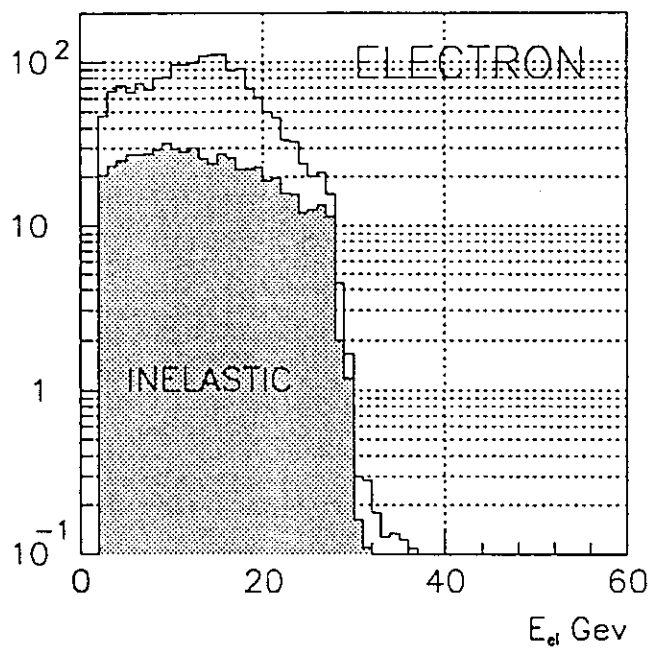
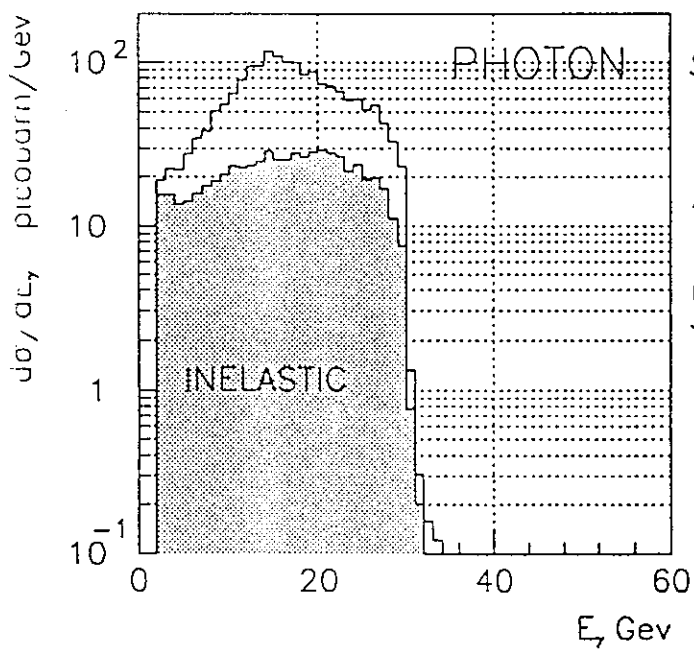


Figure 5

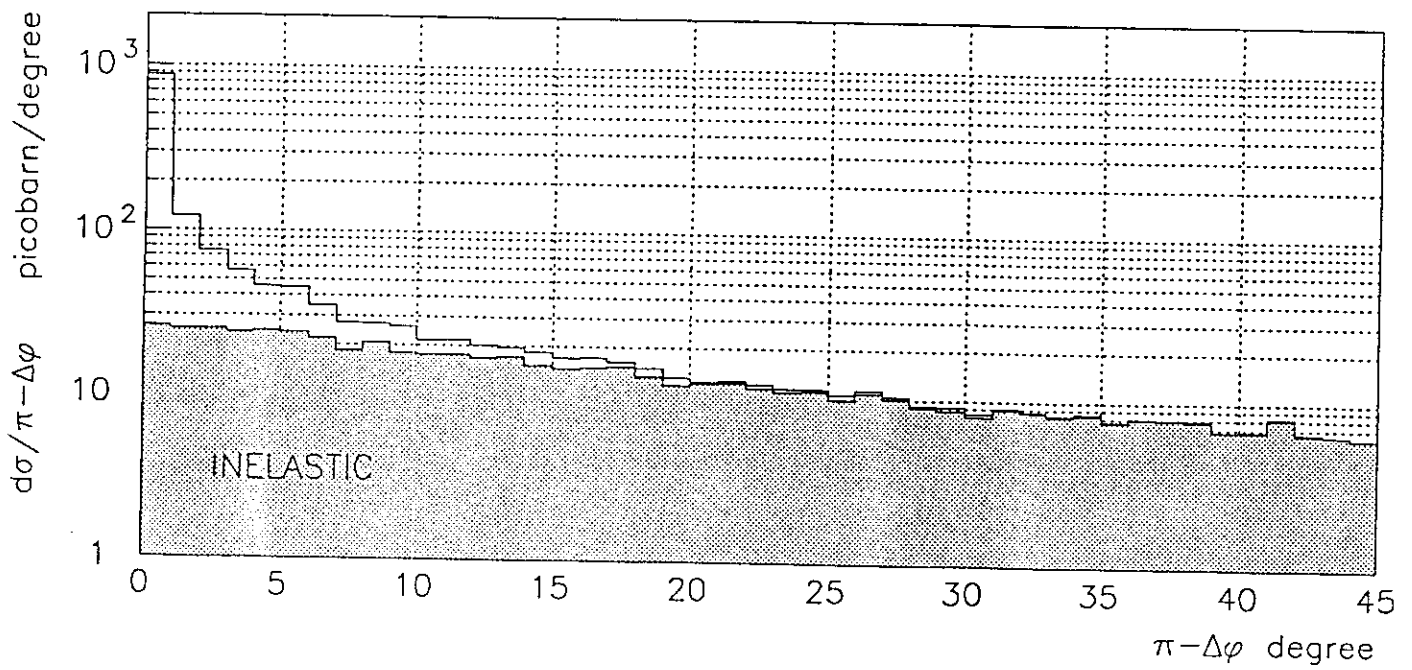
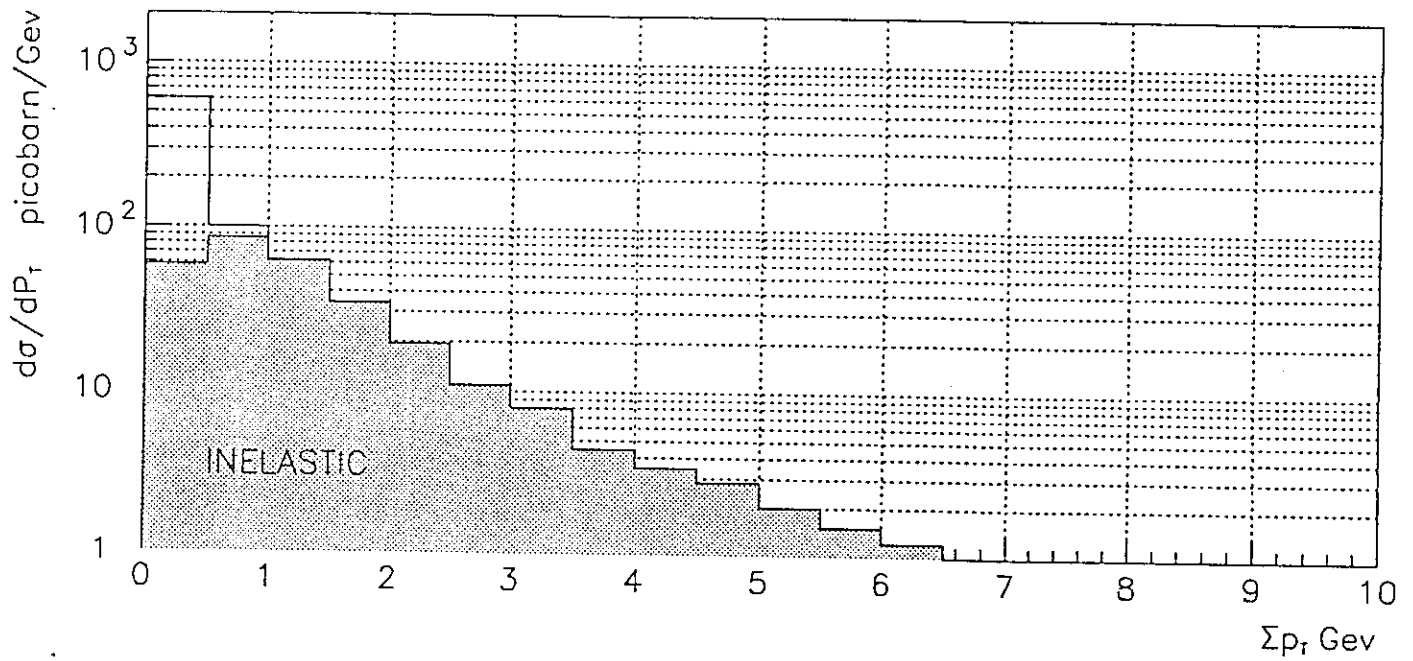


Figure 6

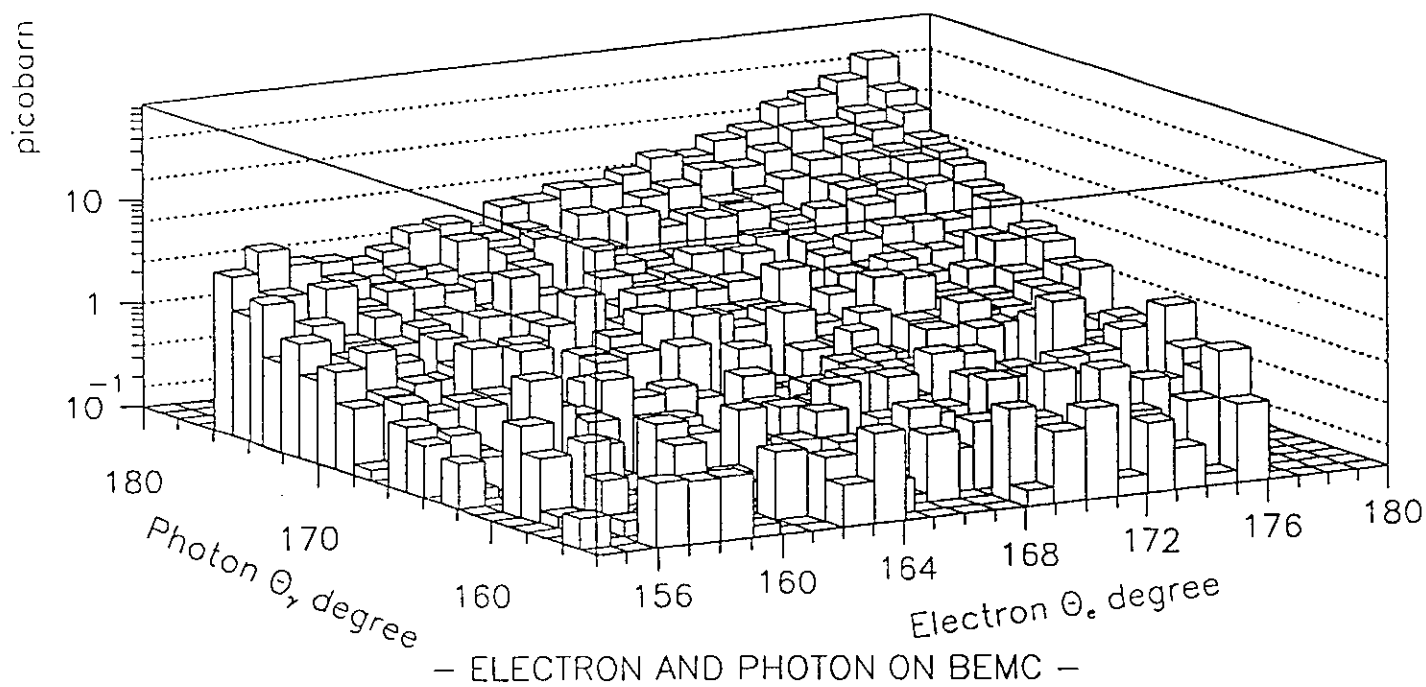
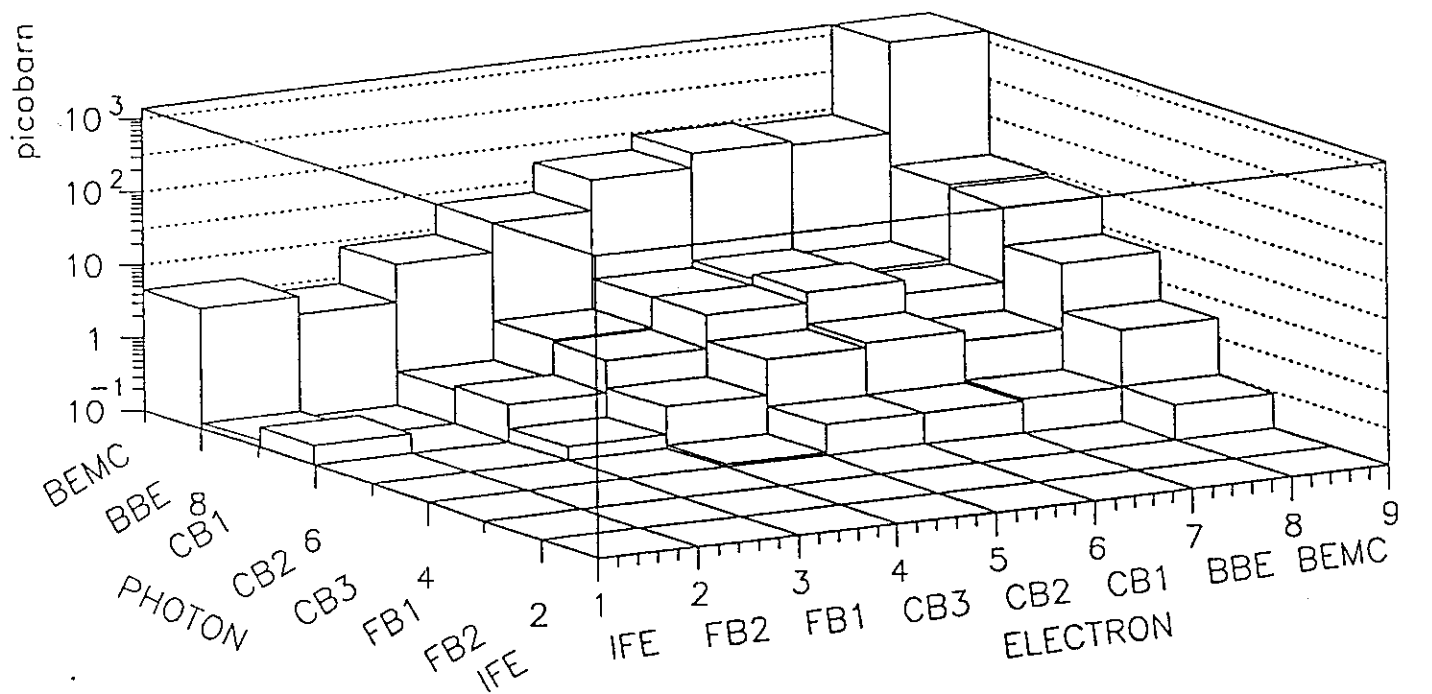


Figure 7